Supporting Information

Bone-Inspired Spatially Specific Piezoelectricity Induces Bone Regeneration

Peng Yu[1, 2] Chengyun Ning[1, 2]*, Yu Zhang[3], Guoxin Tan[4], Zefeng Lin[3], Shaoxiang Liu[3], Xiaolan Wang[3], Haoqi Yang[3], Kang Li[3], Xin Yi[1, 2], Ye Zhu[5], Chuanbin Mao[5,6]*

[1] School of Materials Science and Engineering, Biomedical Engineering Key Laboratory of Guangdong Province, South China University of Technology, Guangzhou, 510641, China

[2] Key Laboratory of Biomedical Sciences and Engineering, South China University of Technology, Guangzhou 510006, China

[3] General Hospital of Guangzhou Military Command of PLA, Guangzhou, 510010, China

[4] Institute of Chemical Engineering and Light Industry, Guangdong University of Technology, Guangzhou, 510006, China

[5] Department of Chemistry and Biochemistry, Stephenson Life Sciences Research Center, University of Oklahoma, Norman OK 73019, USA

[6] School of Materials Science and Engineering, Zhejiang University, Hangzhou, Zhejiang 310027, China

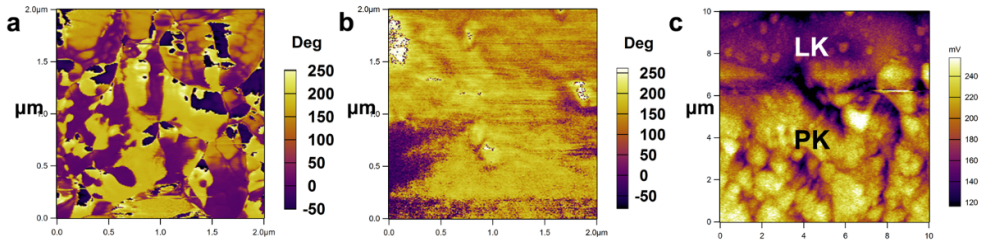

Figure S1. Piezoelectric and surface potential analysis of the relative parts of the MPZs. a-b) Vertical PFM phase mapping of the PK (a) and LK (b) zones. The results indicate that the non-irradiated KNN zone shows better piezoelectricity. c) Scanning Kelvin probe microscopy (SKPM) image of the border of the laser-irradiated zone (upper) and non-irradiated zone (lower) of the MPZs sample, showing that the relative potential of the non-irradiated zone is ~ 59 mV higher than that of the laser-irradiated zone.

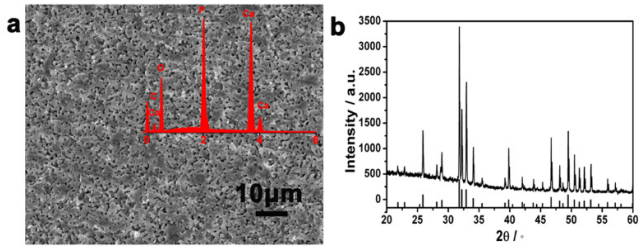

Figure S2. Characterization of the HA control sample. (a) SEM image and EDS spectrum (inlet) of the HA. (c) XRD pattern of HA. The results confirmed the construction of hydroxyapatite ceramic, which was used as the control.

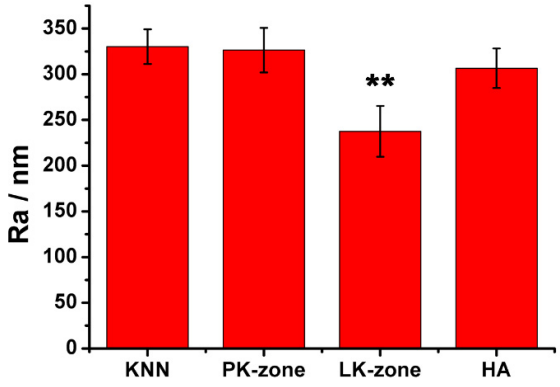

Figure S3. Average surface roughness (Ra) analysis of the MPZs and the control groups acquired by AFM. PK-zone stands for PK-zone of MPZ, and LK-zone stands for LK-zone of MPZ. The results indicate that the roughness of the LK-zone is significantly lower than the other groups while the roughness of the other groups is similar. **, $p<0.01$.

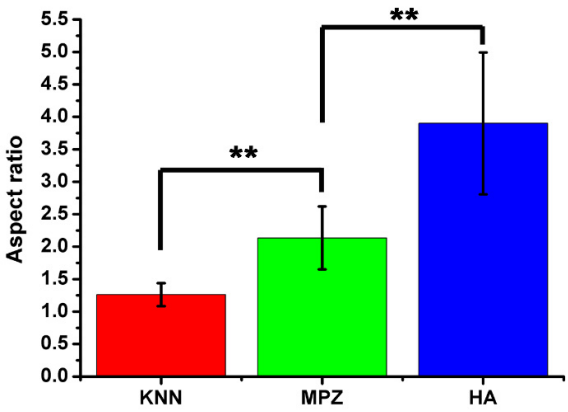

Figure S4. The quantitative aspect ratio analysis of BMSCs cultured on the MPZs and control surfaces for 3 days using the fluorescence images. The assay was repeated twice and expressed as means ± s.d.. Significant differences were determined using a one-way analysis of variance (ANOVA) followed by LSD-t test. (**P <0.01).

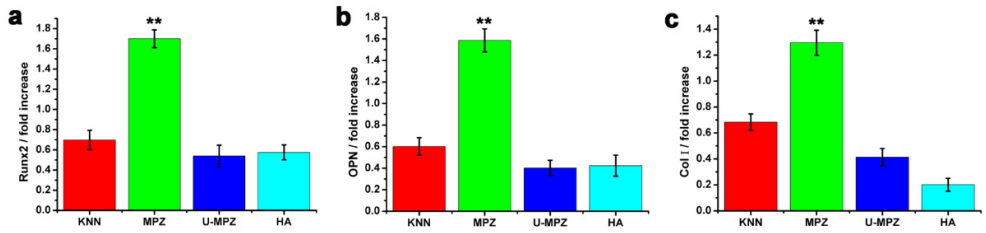

Figure S5. Quantified immunocytochemical analysis of osteogenic proteins (Runx2, Col Ⅰ and OPN) expressed by BMSCs cultured on the different substrates in non-osteogenic growth media for 7 days (Runx2) and 14 days (Col Ⅰ and OPN). The fluorescence intensity of proteins was quantified and later normalized to that of the DAPI staining the cell nuclei in the fluorescence images to obtain fold increase in the production of the proteins. Significant differences were determined using a one-way analysis of variance (ANOVA) followed by LSD-t test. (**) indicates a significant difference at $p < 0.01$ compared to the HA group, n=4.

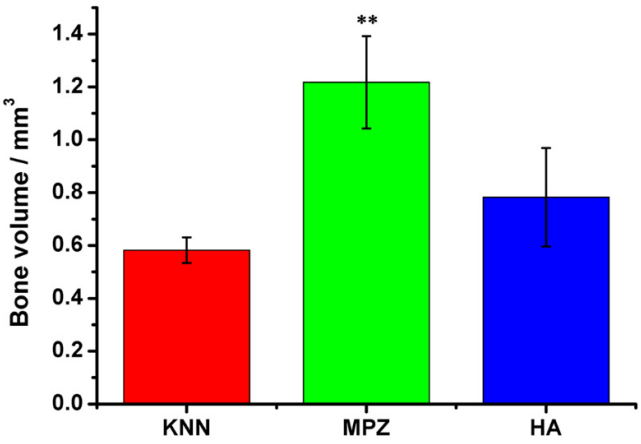

Figure S6. Volume of regenerated bone based on the 3D reconstructed micro-CT images of new bone tissue formed around the implanted KNN, MPZs and HA cylinders after implanted for 4 weeks, respectively. The assay was repeated twice and expressed as means ± s.d.. Significant differences were determined using a one-way analysis of variance (ANOVA) followed by LSD-t test. (**) indicates a significant difference at $p < 0.01$ compared to the HA group, n=4.